

Self-Assessment Module

CPI Body MRI Module 2016

IMAGE-RELATED QUESTIONS

1. An 80-year-old man with a long history of hepatitis B virus infection presents for hepatocellular carcinoma screening. The patient has had multiple prior screening ultrasound examinations with negative results. Three-dimensional (3D) T1-weighted gradient-echo (GRE) (precontrast [Figure 1-1], arterial-phase [Figure 1-2], and delayed-phase [Figure 1-3]), single-shot T2-weighted (Figure 1-4), and diffusion-weighted (inverted grayscale) magnetic resonance (MR) (Figure 1-5) sequences are presented for interpretation. Which *one* of the following is the **CORRECT** diagnosis?
 - A. Focal nodular hyperplasia
 - B. Regenerative nodule
 - C. Dysplastic nodule
 - D. Hepatocellular carcinoma

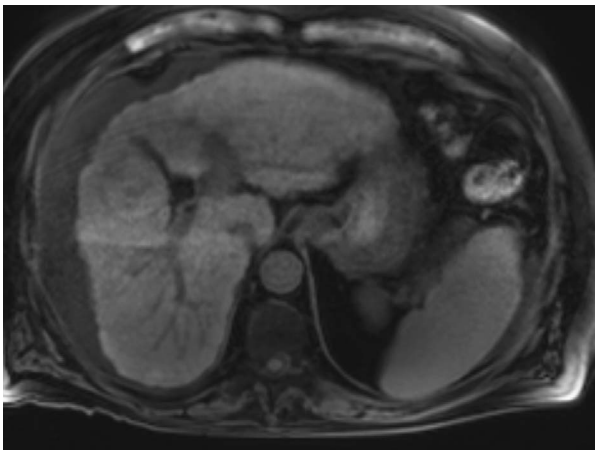


Fig 1-1. Liver. MRI. T1 weighted. Fat suppression. Precontrast. Axial plane.

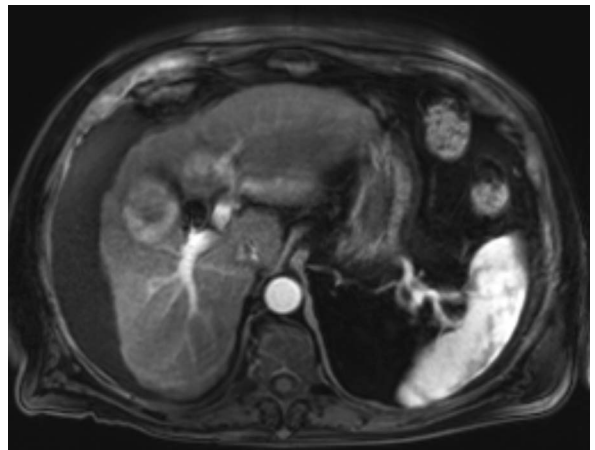


Fig 1-2. Liver. MRI. T1 weighted. Fat suppression. Contrast enhancement. Arterial phase. Axial plane.

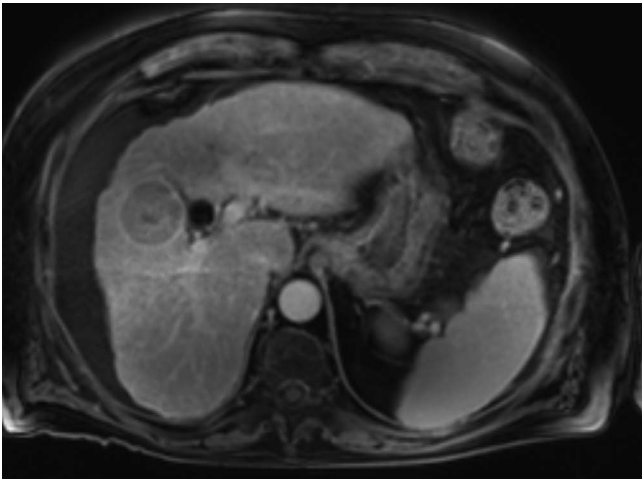


Fig 1-3. Liver. MRI. T1 weighted. Fat suppression. Contrast enhancement. Delayed phase. Axial plane.

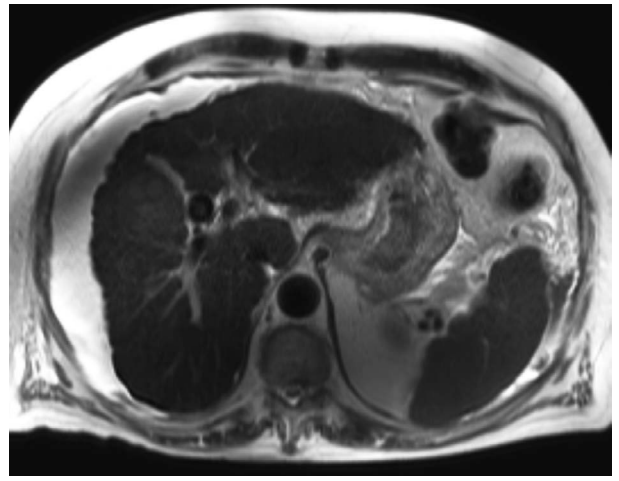


Fig 1-4. Liver. MRI. T2 weighted. Single shot. Axial plane.

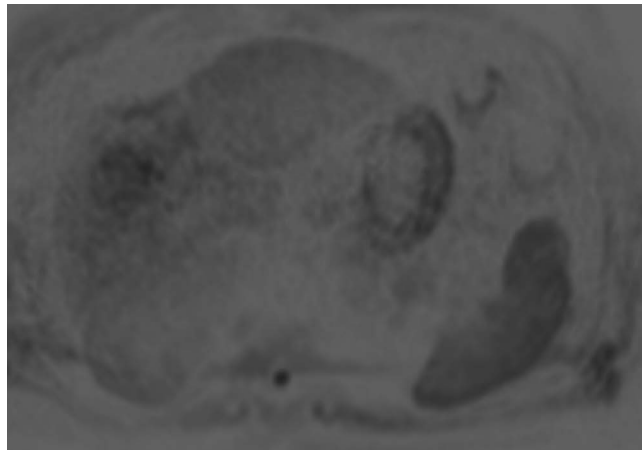


Fig 1-5. Liver. MRI. Diffusion weighted imaging (DWI) (inverted grayscale). b=500. Axial plane.

2. A 60-year-old man with a history of alcohol abuse and hepatitis C virus infection presents with severe abdominal pain. Ultrasound demonstrated changes consistent with end-stage chronic liver disease with ascites, and the patient underwent paracentesis. The serum α fetoprotein level was normal. However, the patient continued to have pain, and a magnetic resonance image (MRI) was obtained. Three-dimensional T1-weighted GRE (precontrast [Figure 2-1], arterial-phase [Figure 2-2], and delayed-phase [Figure 2-3]), single-shot T2-weighted (Figure 2-4), and diffusion-weighted (inverted grayscale) (Figure 2-5) sequences are presented for interpretation. Which *one* of the following is the **CORRECT** diagnosis?
- A. Intrahepatic cholangiocarcinoma with bland thrombus in the left portal vein
 - B. Infiltrative hepatocellular carcinoma with tumor thrombus in the left portal vein
 - C. Focal hepatic inflammation with bland thrombus in the left portal vein
 - D. Confluent fibrosis with tumor thrombus in the left portal vein

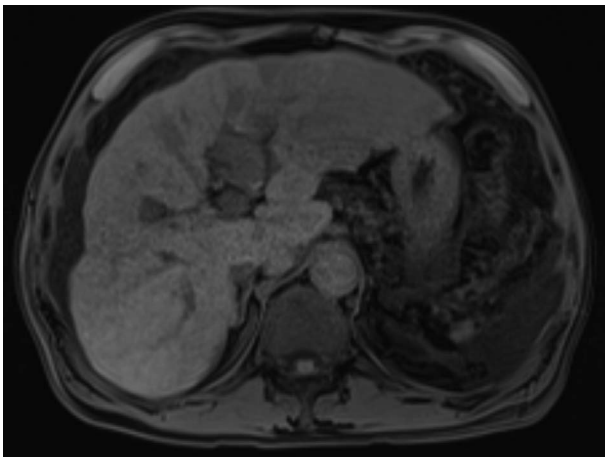


Fig 2-1. Liver. MRI. T1 weighted. Fat suppression. Precontrast. Axial plane.

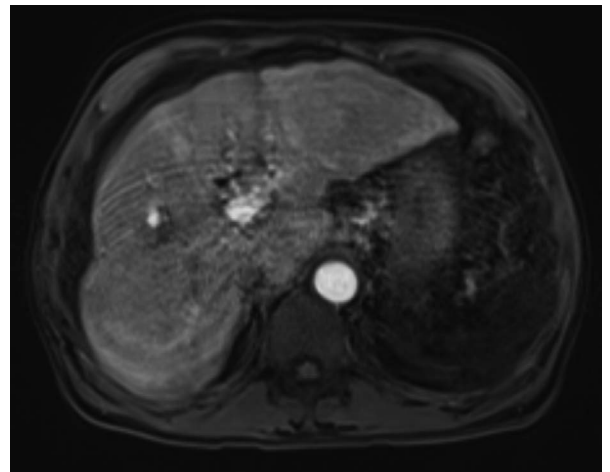


Fig 2-2. Liver. MRI. T1 weighted. Fat suppression. Contrast enhancement. Arterial phase. Axial plane.

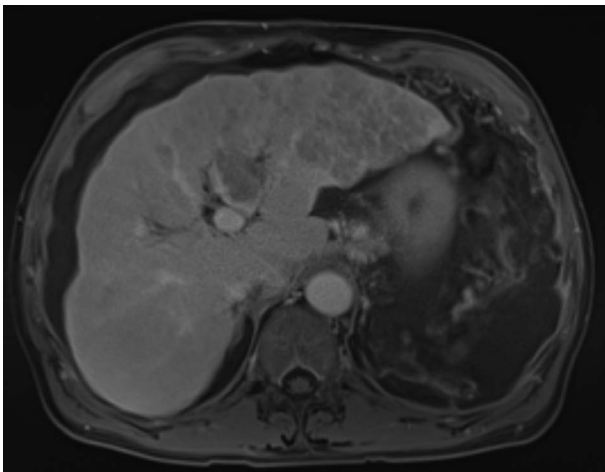


Fig 2-3. Liver. MRI. T1 weighted. Fat suppression. Contrast enhancement. Delayed phase. Axial plane.

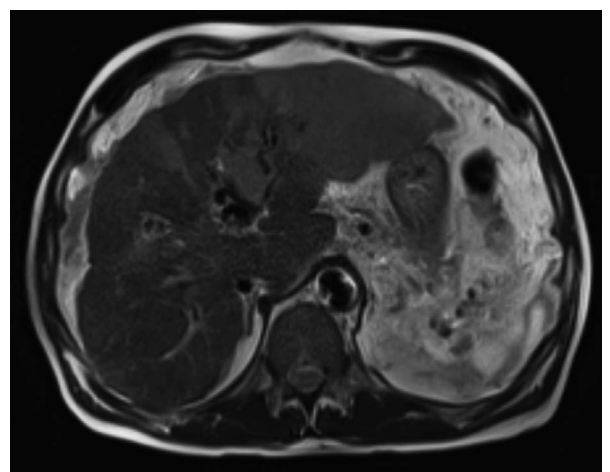


Fig 2-4. Liver. MRI. T2 weighted. Single shot. Axial plane.

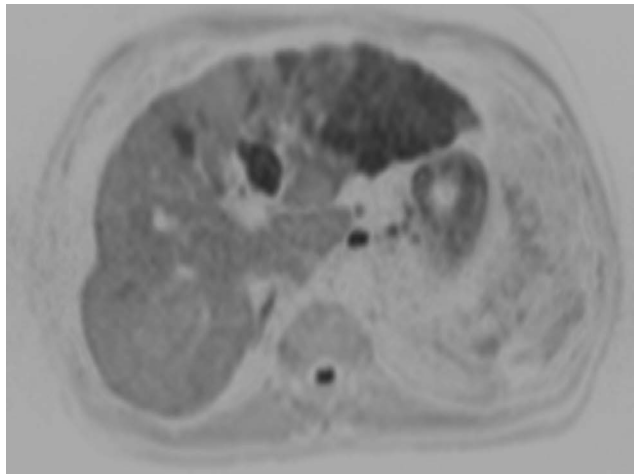


Fig 2-5. Liver. MRI. DWI (inverted grayscale).
 $b=500$. Axial plane.

3. A 27-year-old woman taking oral contraceptives presents with an enhancing hepatic lesion identified incidentally on computed tomography (CT). MRI was performed for further characterization. Three-dimensional T1-weighted GRE (precontrast [Figure 3-1], arterial-phase [Figure 3-2], and delayed-phase [Figure 3-3]), fat-saturated single-shot T2-weighted (Figure 3-4), and diffusion-weighted (inverted grayscale) (Figure 3-5) sequences are presented for interpretation. Which *one* of the following is the **CORRECT** diagnosis?
- A. Hepatic adenoma
 - B. Hepatocellular carcinoma
 - C. Focal nodular hyperplasia
 - D. Hypervascular metastasis

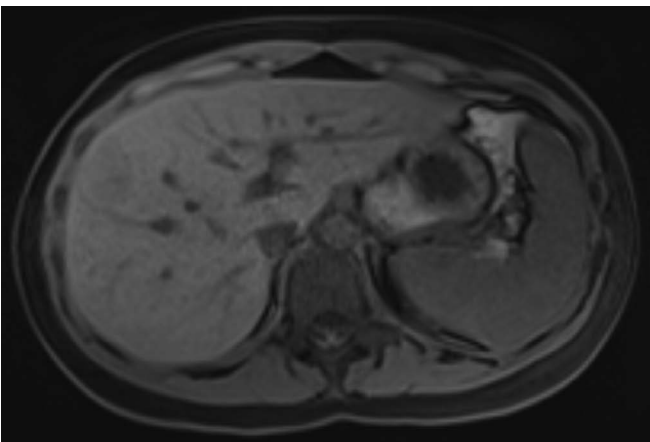


Fig 3-1. Liver. MRI. T1 weighted. Fat suppression.
Precontrast. Axial plane.

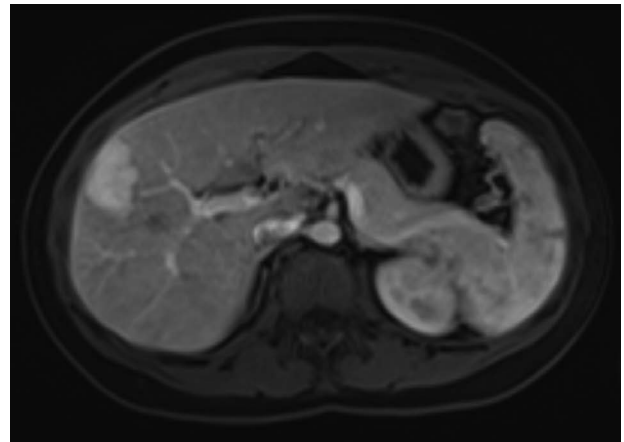


Fig 3-2. Liver. MRI. T1 weighted. Fat suppression.
Contrast enhancement. Arterial phase. Axial plane.

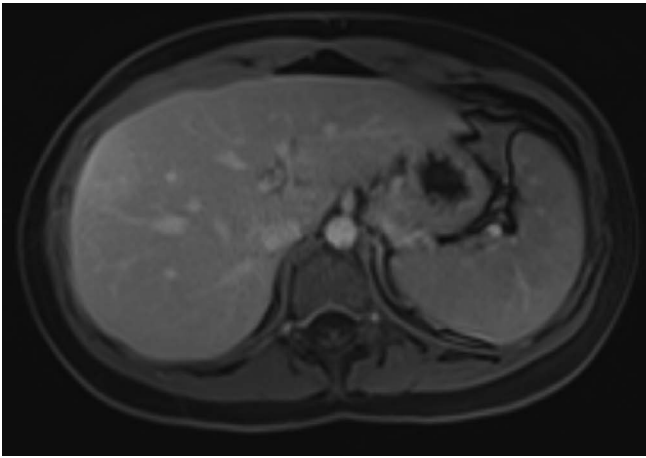


Fig 3-3. Liver. MRI. T1 weighted. Fat suppression. Contrast enhancement. Delayed phase. Axial plane.

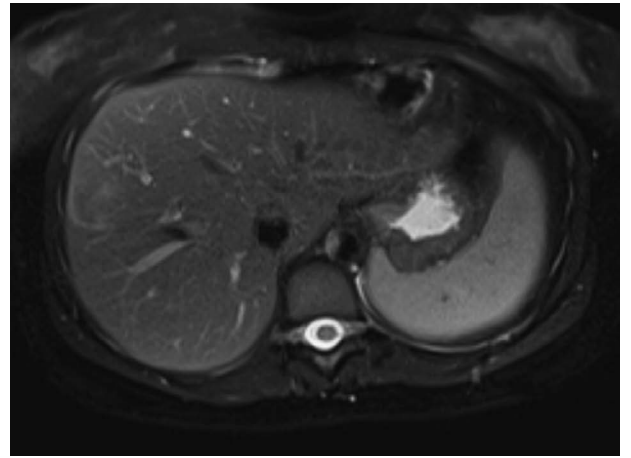


Fig 3-4. Liver. MRI. T2 weighted. Single shot. Fat suppression. Axial plane.

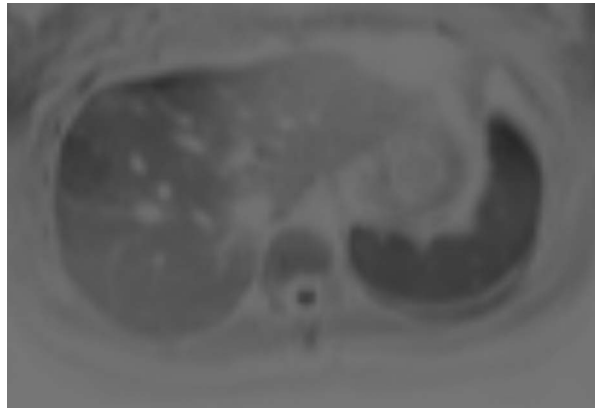


Fig 3-5. Liver. MRI. DWI (inverted grayscale). b=500. Axial plane.

40. Which MR sequence is **MOST** critical for detection of acute inflammatory changes in the patients presenting with acute abdominopelvic pain?
- A. Fat-suppressed single-shot T2-weighted sequence
 - B. Non-fat-saturated single-shot T2-weighted images
 - C. Balanced steady-state free precession
 - D. Precontrast 3D fat-suppressed GRE T1-weighted sequences
41. Regarding noninvasive staging of endometrial cancer, which *one* of the following is **CORRECT**?
- A. Pelvic ultrasound is the imaging modality of choice for staging of endometrial cancer.
 - B. The depth of myometrial invasion is an important prognostic factor.
 - C. MRI does not reliably demonstrate tumor extension into the adjacent junctional zone.
 - D. Administration of intravenous contrast has no added value in staging endometrial cancer with MRI.
42. Regarding endometrial cancer, which *one* of the following is **CORRECT**?
- A. It commonly occurs in young patients.
 - B. Endometrial cancer always invades the myometrium.
 - C. The incidence of endometrial cancer in young women is associated with a high body mass index.
 - D. A safe fertility-sparing approach in endometrial cancer treatment in young women is not feasible.
43. In a 68-year-old man with no prior history of prostate cancer, a rising or persistently elevated serum prostate-specific antigen level, and several negative transrectal ultrasound-guided prostate biopsies, which of the following is the **MOST** appropriate *next* step for further imaging evaluation, based on the American College of Radiology Appropriateness Criteria®?
- A. Contrast-enhanced prostate MRI
 - B. Transrectal color Doppler ultrasound to select a biopsy target
 - C. CT of the abdomen and pelvis
 - D. Contrast-enhanced pelvic MRI to select a directed biopsy target
44. Regarding differentiating epithelial thymic neoplasms from thymic hyperplasia with MR imaging, which *one* of the following is **CORRECT**?
- A. The shape of the thymic gland is the most reliable MR characteristic in differentiating thymoma from thymic hyperplasia.
 - B. Decreased signal on out-of-phase GRE T1-weighted imaging is diagnostic of thymic hyperplasia.
 - C. T2 signal intensity is accurate for differentiating thymoma from thymic hyperplasia.
 - D. The visualization of a low-signal capsule on T2-weighted imaging is indicative of thymic hyperplasia.

Answer Key

CPI Body MRI Module 2016

- | | |
|-------|-------|
| 1. D | 26. C |
| 2. B | 27. B |
| 3. C | 28. C |
| 4. A | 29. B |
| 5. D | 30. C |
| 6. B | 31. A |
| 7. A | 32. D |
| 8. B | 33. B |
| 9. B | 34. B |
| 10. C | 35. A |
| 11. C | 36. D |
| 12. A | 37. B |
| 13. B | 38. A |
| 14. C | 39. B |
| 15. C | 40. A |
| 16. C | 41. B |
| 17. D | 42. C |
| 18. B | 43. D |
| 19. B | 44. B |
| 20. D | 45. B |
| 21. D | 46. C |
| 22. B | 47. B |
| 23. A | 48. A |
| 24. B | 49. D |
| 25. D | 50. D |

Rationales and References

Answer 1 is D.

A focal lesion in the right hepatic lobe (Figures 1-1, 1-2, 1-3, 1-4, and 1-5) demonstrates arterial enhancement (Figure 1-2) and washout (Figure 1-3), with a delayed enhancing capsule. The T2 signal of the mass is similar or slightly elevated compared to background liver intensity. Mild restricted diffusion (Figure 1-5) is present. In a patient with chronic liver disease, the imaging features of this case are diagnostic for hepatocellular carcinoma (HCC).



Fig 1-1. Hepatocellular carcinoma (HCC). Annotated. Liver. MRI. T1 weighted. Fat suppression. Precontrast. Axial plane. An arrow points to a focal lesion in the right hepatic lobe.



Fig 1-2. HCC. Annotated. Liver. MRI. T1 weighted. Fat suppression. Contrast enhancement. Arterial phase. Axial plane. An arrow points to a focal lesion in the right hepatic lobe. There is arterial phase enhancement.



Fig 1-3. HCC. Annotated. Liver. MRI. T1 weighted. Fat suppression. Contrast enhancement. Delayed phase. Axial plane. An arrow points to the focal lesion in the right hepatic lobe. There is washout and a delayed enhancing capsule.

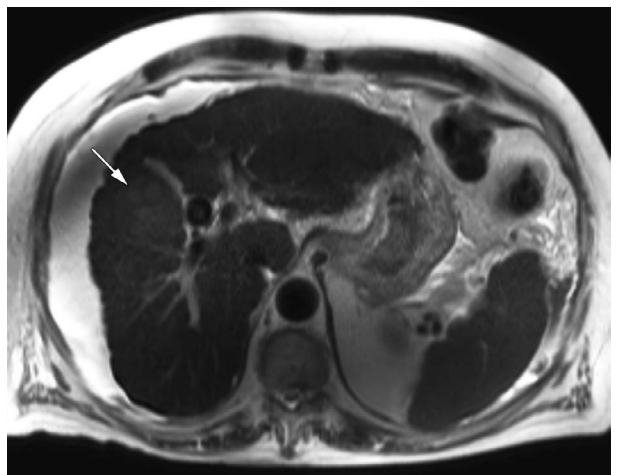


Fig 1-4. HCC. Annotated. Liver. MRI. T2 weighted. Single shot. Axial plane. An arrow points to a focal lesion in the right hepatic lobe. The tumor is not very conspicuous on T2-weighted imaging, with only mildly increased signal.

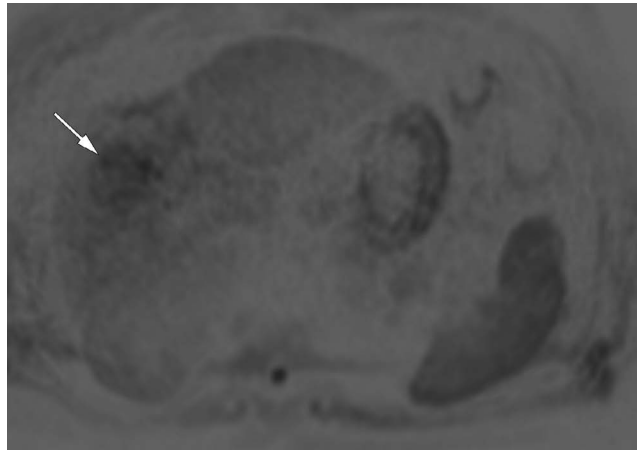


Fig 1-5. HCC. Annotated. Liver. MRI. DWI (inverted grayscale). $b=500$. Axial plane. An arrow points to a focal lesion in the right hepatic lobe.

Magnetic resonance imaging (MRI) is highly sensitive and specific for the detection of HCC. HCCs demonstrate heterogeneous enhancement on arterial-phase images, with washout (becoming hypointense to background liver) and a thick, enhancing capsule on delayed-phase images. The T2 signal is variable, though it may be mildly elevated. The DWI signal is also variable, with some HCCs demonstrating little or no restricted diffusion. Some HCCs (especially more aggressive tumors), however, will demonstrate restricted diffusion.

Although ultrasound (US) is a commonly employed imaging method for HCC screening in patients with chronic liver disease, US is relatively insensitive for imaging early-stage tumors compared with MRI. The goal of screening is to identify early-stage disease that falls within transplant criteria, ie, either a single tumor smaller than 5 cm or no more than 3 tumors that are all 3 cm or smaller (Milan criteria). Transplantation is the single most effective therapy for treating both the patient's tumor and their underlying chronic liver disease. Accurate screening is required for optimum therapeutic interventions.

Option A is not correct.

Focal nodular hyperplasia (FNH) is not a diagnostic consideration in a patient with a history of chronic liver disease as in the test patient. In addition, FNH shows a typical pattern of small, enhancing nodules within and along the edge of the lesion. FNH will not demonstrate washout (become hypointense to background liver), which is a feature seen in HCC. In contrast, FNH tends to fade and become isointense (or remain slightly hyperintense) to background liver on delayed-phase images.

Option B is not correct.

Regenerative nodules are islands of normal hepatic parenchyma surrounded by fibrosis. As such, these nodules have a vascular supply similar to that of normal liver and do not show increased arterial enhancement compared with the enhancement of the remainder of the liver parenchyma. Regenerative nodules also do not demonstrate elevated T2 signal or restricted diffusion, which are seen to a mild extent in this patient.

Option C is not correct.

As nodules in the setting of chronic liver disease become more dysplastic, they recruit more unpaired hepatic arteries (ie, arteries not paired with a bile duct) and begin to lose portal supply. For this reason, dysplastic nodules manifest on imaging as nodules with increased arterial enhancement compared with background hepatic parenchyma, but they do not yet demonstrate the washout that is typical for HCC.

Reference(s):

- Becker-Weidman DJ, Kalb B, Sharma P, et al. Hepatocellular carcinoma lesion characterization: single-institution clinical performance review of multiphase gadolinium-enhanced MR imaging--comparison to prior same-center results after MR systems improvements. *Radiology*. 2011;261:824-833.
- Chou CT, Chou JM, Chang TA, et al. Differentiation between dysplastic nodule and early-stage hepatocellular carcinoma: the utility of conventional MR imaging. *World J Gastroenterol*. 2013;19:7433-7439.
- Lee YJ, Lee JM, Lee JS, et al. Hepatocellular carcinoma: diagnostic performance of multidetector CT and MR imaging--a systematic review and meta-analysis. *Radiology*. 2015;275:97-109.
- Mazzaferro V, Regalia E, Doci R, et al. Liver transplantation for the treatment of small hepatocellular carcinomas in patients with cirrhosis. *New Engl J Med*. 1996;334:693-699.
- Yu NC, Chaudhari V, Raman SS, et al. CT and MRI improve detection of hepatocellular carcinoma, compared with ultrasound alone, in patients with cirrhosis. *Clin Gastroenterol Hepatol*. 2011;9:161-167.

Answer 2 is B.

Ill-defined, heterogeneous arterial enhancement is noted involving the entire lateral segment of the left hepatic lobe. This area also shows washout on postcontrast delayed-phase imaging (Figures 2-1, 2-2, and 2-3, arrows). There is abnormal, moderately elevated T2 signal (Figure 2-4, arrow) and restricted diffusion (Figure 2-5, arrow). Note also that the thrombus in the left portal vein (Figures 2-1, 2-2, 2-3, 2-4, and 2-5, arrowheads) has imaging features identical to the tumor replacing the left lateral segment of the liver. These features are diagnostic of infiltrative hepatocellular carcinoma (I-HCC), with tumor thrombus filling the left portal vein.

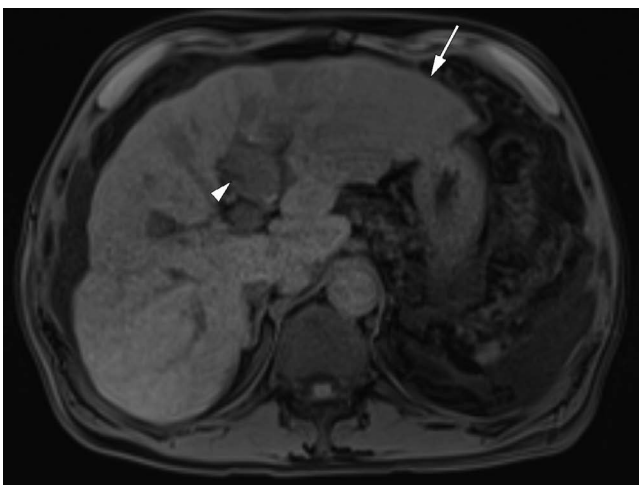


Fig 2-1. Infiltrative hepatocellular carcinoma (I-HCC). Annotated. Liver. MRI. T1 weighted. Fat suppression. Precontrast. Axial plane. An arrow points to an I-HCC. An arrowhead points to tumor thrombus in the left portal vein. The mass is seen in the lateral segment of the left hepatic lobe. It is lower in intensity than the remainder of the liver.

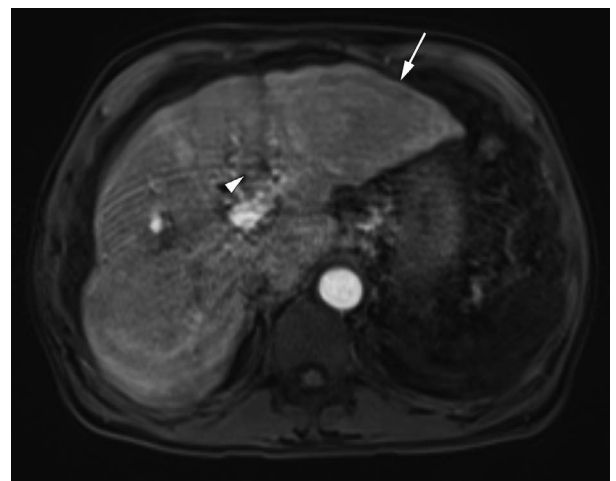


Fig 2-2. I-HCC. Annotated. Liver. MRI. T1 weighted. Fat suppression. Contrast enhancement. Arterial phase. Axial plane. An arrow points to an I-HCC. An arrowhead points to tumor thrombus in the left portal vein.

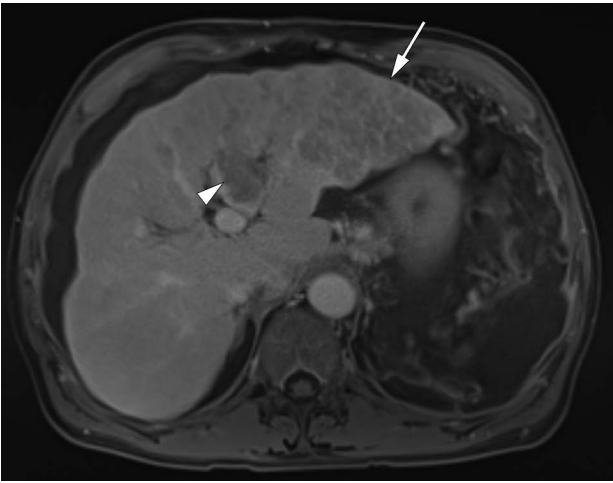


Fig 2-3. I-HCC. Annotated. Liver. MRI. T1 weighted. Fat suppression. Contrast enhancement. Delayed phase. Axial plane. An arrow points to the low-intensity I-HCC in the lateral segment of the left lobe of the liver. An arrowhead points to tumor thrombus in the left portal vein.

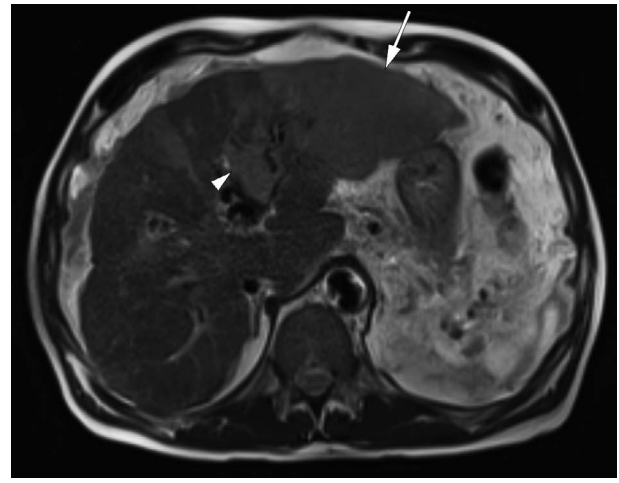


Fig 2-4. I-HCC. Annotated. Liver. MRI. T2 weighted. Single shot. Axial plane. An arrow points to I-HCC. An arrowhead points to tumor thrombus in the left portal vein.

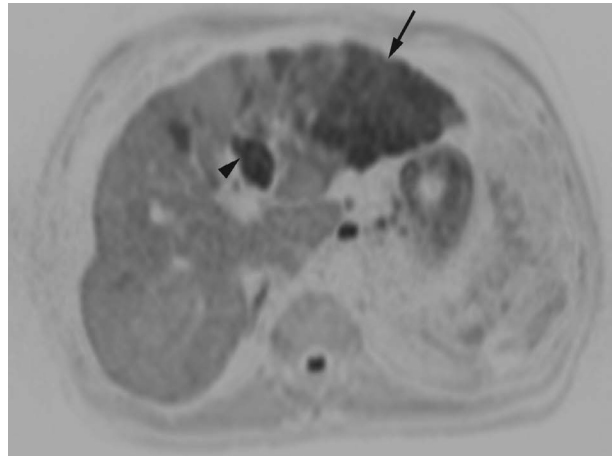


Fig 2-5. I-HCC. Annotated. Liver. MRI. DWI (inverted grayscale). b=500. Axial plane. An arrow points to the area of restricted diffusion of the left hepatic lobe lateral segment's I-HCC. An arrowhead points to tumor thrombus in the left portal vein.

I-HCC is a very aggressive form of tumor that carries a markedly poor prognosis. Unlike the more common focal type of hepatocellular carcinoma (HCC), I-HCC demonstrates variable arterial enhancement and washout and may be relatively inconspicuous on standard pre- and postcontrast T1-weighted 3D gradient-echo (GRE) sequences. However, I-HCC demonstrates markedly abnormal T2 signal and will also demonstrate restricted diffusion, features that are not always seen with conventional focal HCC. I-HCC is also very frequently associated with a tumor thrombus that expands portal vein branches. The distinction between bland and tumor thrombi is relatively straightforward and relies on demonstrating enhancement within the portal thrombus, matching the enhancement pattern of the primary infiltrative tumor. Note that T2 signal and diffusion characteristics of the tumor thrombus are also similar to those of the infiltrative parenchymal tumor.

Option A is not correct.

The images of the test patient have background changes of chronic liver disease. One can see a nodular morphology of the liver with hypertrophy of the left lateral segment. In addition, the infiltrative tumor in the left lateral segment demonstrates washout on delayed-phase images. The enhancing tumor thrombus within the left portal system expands the portal vein, which is a characteristic of HCC. An intrahepatic cholangiocarcinoma, on the other hand, typically constricts and obliterates the portal vein.

Option C is not correct.

The thrombus within the left portal vein clearly demonstrates enhancement, a feature of tumor thrombus and not bland thrombus.

Option D is not correct.

Confluent fibrosis is frequently seen with background chronic liver disease, but it is a uniform process that demonstrates homogeneous, delayed enhancement. In the test patient, the region of abnormal signal in the left lateral segment is markedly heterogeneous and demonstrates washout on delayed-phase images. In addition, tumor thrombus is not seen with isolated confluent fibrosis.

Reference(s):

Kanematsu M, Semelka RC, Leonardou P, Mastropasqua M, Lee JK. Hepatocellular carcinoma of diffuse type: MR imaging findings and clinical manifestations. *J Magn Reson Imaging*. 2003;18:189-195.

Reynolds AR, Furlan A, Fetzer DT, et al. Infiltrative hepatocellular carcinoma: what radiologists need to know. *RadioGraphics*. 2015;35:371-386.

Rosenkrantz AB, Lee L, Matza BW, Kim S. Infiltrative hepatocellular carcinoma: comparison of MRI sequences for lesion conspicuity. *Clin Radiol*. 2012;67:e105-e111.

Answer 3 is C.

A focal lesion in the right hepatic lobe (Figures 3-1, 3-2, 3-3, 3-4, and 3-5) demonstrates nodular arterial enhancement (Figure 3-1) and becomes near-isointense to background liver on delayed-phase imaging (Figure 3-3). The lesion is isointense to background liver on precontrast T1-weighted (Figure 3-1), single-shot T2-weighted (Figure 3-4) and diffusion-weighted (Figure 3-5) images. There are no changes of background chronic liver disease, which decreases concern for HCC. Regardless, these imaging findings are diagnostic for focal nodular hyperplasia (FNH).

FNH is a hamartomatous hepatic lesion containing disorganized arrangements of hepatocytes and bile ductules. Pathologists often refer to FNH as a “localized cirrhosis” because of the relatively normal-appearing hepatic tissue surrounded by fibrotic bands. On MRI, FNH demonstrates signal features similar to those of background hepatic parenchyma on all sequences except the parenchymal arterial-phase sequence, where FNH demonstrates avid arterial enhancement.

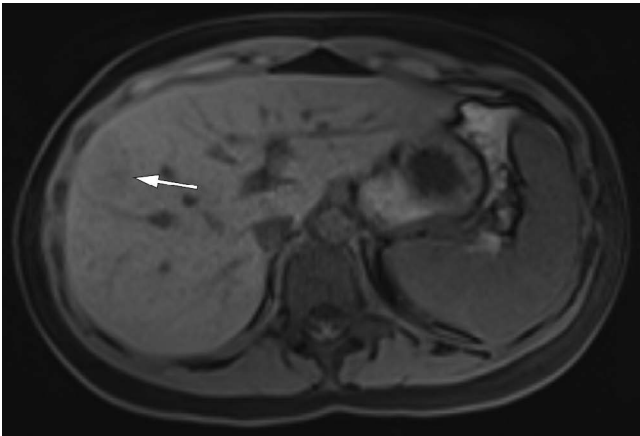


Fig 3-1. Focal nodular hyperplasia (FNH). Annotated. Liver. MRI. T1 weighted. Fat suppression. Precontrast. Axial plane. An arrow points to a right hepatic lobe mass, which proved to be an FNH.

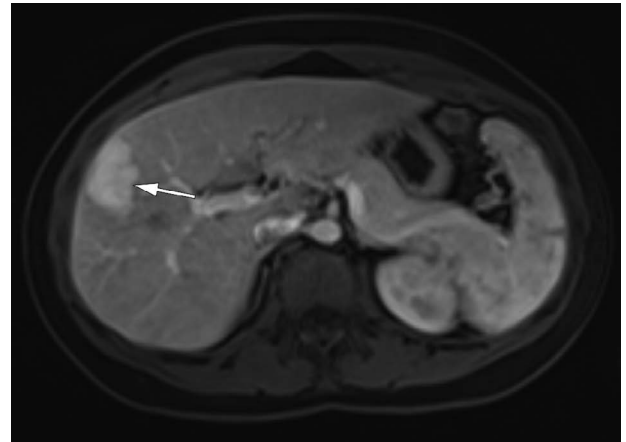


Fig 3-2. FNH. Annotated. Liver. MRI. T1 weighted. Fat suppression. Contrast enhancement. Arterial phase. Axial plane. An arrow points to a right hepatic lobe mass, which shows nodular arterial enhancement. Avid arterial-phase enhancement is characteristic for an FNH.

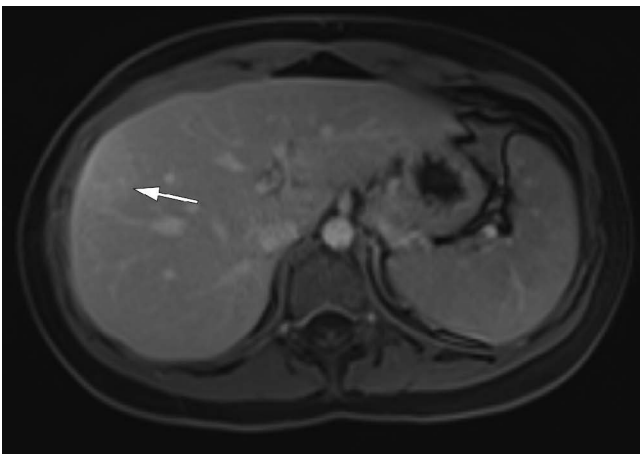


Fig 3-3. FNH. Annotated. Liver. MRI. T1 weighted. Fat suppression. Contrast enhancement. Delayed phase. Axial plane. On delayed-phase imaging, the mass (arrow) becomes near isointense to background liver, consistent with an FNH.

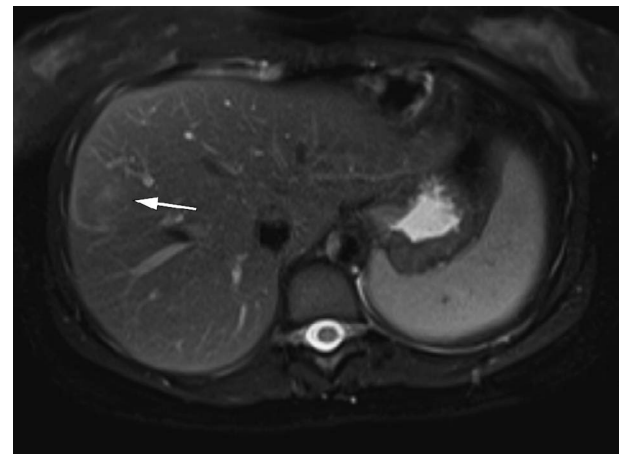


Fig 3-4. FNH. Annotated. Liver. MRI. T2 weighted. Single shot. Fat suppression. Axial plane. An arrow points to the right hepatic lobe mass. It is isointense to the background liver, consistent with FNH.

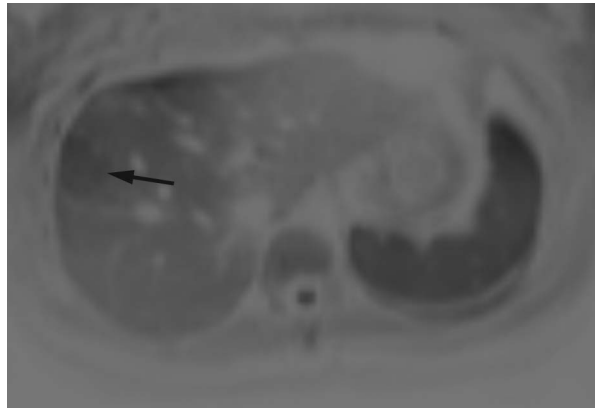


Fig 3-5. FNH. Annotated. Liver. MRI. DWI (inverted grayscale). b=500. Axial plane. An arrow points to the liver mass in the right lobe. Intensity of the mass is similar to that of the background liver.

The internal architecture of FNH is also characteristic. It is composed of tiny enhancing nodules both within and along the edge of the lesion. Thin septa are noted separating the nodules within the lesion, correlating to the fibrotic bands noted on histopathology. A central scar may be seen. However, this is not universally present and is not required for the diagnosis. Both FNH and adenoma are seen more frequently with oral contraceptive therapy. These masses “scar down,” ie, disappear when the patient goes through menopause.

Option A is not correct.

Hepatic adenomas are hepatic neoplasms composed of sheets of hepatocytes, containing a relative lack of bile ductules compared with FNH. Adenomas more commonly contain internal lipid (demonstrated on in-phase and out-of-phase imaging) and hemorrhage. Non-lipid-containing, nonhemorrhagic adenomas demonstrate a more uniform ground-glass arterial enhancement and lack the nodularity and internal architecture findings that are characteristic of FNH. Without hemorrhage or internal heterogeneity, hepatic adenomas are benign lesions that can be followed with noninvasive imaging and do not typically require resection when uncomplicated.

Option B is not correct.

The test images do not show background chronic liver disease. While hepatocellular carcinoma (HCC) may occur in an otherwise normal liver, this would be unusual. In addition, HCC demonstrates arterial enhancement and delayed washout with a delayed-enhancing capsule; the latter 2 features are absent in this patient.

Option D is not correct.

Even if the test patient had a history of hypervascular malignancy, the imaging features of this lesion are not in keeping with metastatic disease. This lesion blends into the background on both precontrast T1- and T2-weighted sequences, which is characteristic of FNH. Metastatic disease is hypointense on precontrast T1-weighted sequences, contrasting well with the background hyperintense normal hepatic parenchyma. Metastatic lesions (especially most hypervascular metastases) are moderately hyperintense on T2-weighted images (similar to spleen) and may show restricted diffusion. They tend to be multiple in number. None of these features are seen in the test case.

Reference(s):

Cogley JR, Miller FH. MR imaging of benign focal liver lesions. *Radiol Clin North Am.* 2014;52:657-682.

Answer 30 is C.

Aneurysmal dilatation of the ascending aorta in the test patient is centered in the aortic root. There is involvement of the aortic annulus and effacement of the sinotubular junction, resulting in the characteristic “tulip bulb” appearance of annuloaortic ectasia. This configuration of the ascending aortic dilation is associated with underlying cystic medial necrosis. The underlying histologic findings include a loss of elastic and muscle fibers in the aortic media, with accumulation of mucopolysaccharides that result in cyst-like spaces between the muscle fibers, weakening the aortic wall. Cystic medial necrosis is seen in connective tissue disorders, such as Marfan syndrome, as well as in patients with bicuspid aortic valves (bicuspid aortopathy). This patient had Loeys-Dietz syndrome.

Option A is not correct.

Figure 30-2 demonstrates that the aortic valve is clearly tricuspid. Bicuspid aortic valves are often associated with cystic medial necrosis, and the resulting aortic dilatation can often take the form of annuloaortic ectasia, similar to that seen in connective tissue disorders, such as Marfan syndrome.

Option B is not correct.

Figure 30-3 demonstrates that the aortic valve is normal in appearance and the valve leaflets are not thickened or calcified. Also, ascending aortic aneurysms related to age-related aortic stenosis typically spare the annulus and aortic root, instead causing fusiform dilatation of the tubular ascending aorta.

Option D is not correct.

Figures 30-1 and 30-3 demonstrate aortic dilatation that is centered in the aortic root, involving the annulus and effacing the sinotubular junction. Ascending aortic aneurysms related to hypertension and atherosclerosis typically spare the annulus and aortic root and, instead, cause fusiform dilation of the tubular ascending aorta.

Reference(s):

Isselbacher EM. Thoracic and abdominal aortic aneurysms. *Circulation*. 2005;111:816-828.

Kimura-Hayama ET, Meléndez G, Mendizábal AL, Meave-González A, Zambrana GF, Corona-Villalobos CP. Uncommon congenital and acquired aortic diseases: role of multidetector CT angiography. *RadioGraphics*. 2010;30:79-98.

Nataf P, Lansac E. Dilation of the thoracic aorta: medical and surgical management. *Heart*. 2006;92:1345-1352.

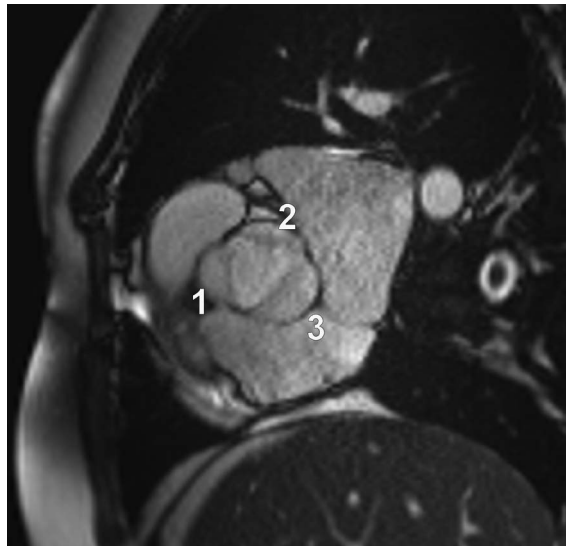


Fig 30-2. Tricuspid aortic valve. Annotated. Heart. MRI. Steady-state free precession. Contrast enhancement. Axial plane. Level through the aortic valve. 1, 2, 3 = aortic valve cusps.

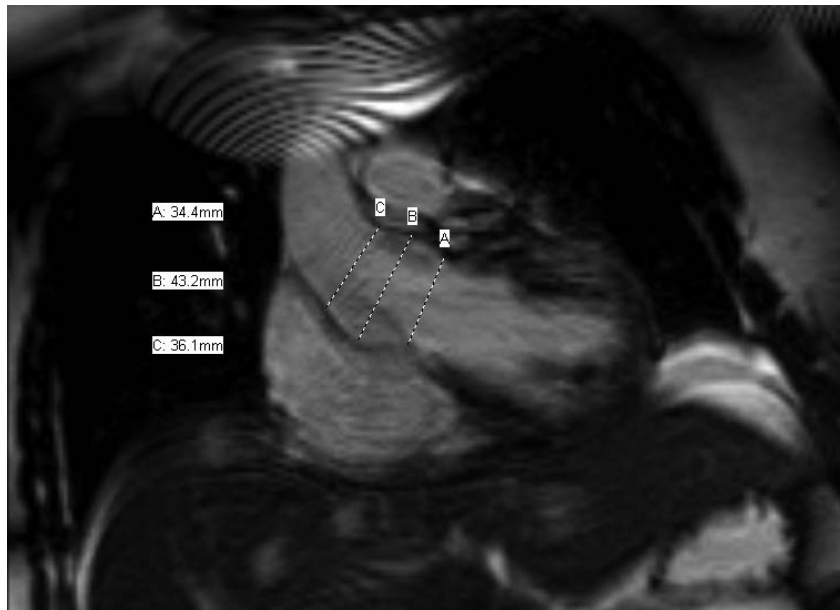


Fig 30-3. Normal aortic valve. Annotated. Heart. MRI. Steady-state free precession. Coronal plane. Level through the aortic root.

Answer 31 is A.

There is a large filling defect in the otherwise contrast-filled pulmonary arteries (Figures 31-2 and 31-3), consistent with an acute saddle pulmonary embolism (PE). The filling defect does not demonstrate any appreciable enhancement on the postcontrast images (Figures 31-2 and 31-3). In addition, the filling defect is located centrally within the vessel, as would be expected in acute PE. Chronic PE usually has a more peripheral location, forming obtuse angles with the wall of the vessel. These pulmonary clots usually form in the deep veins of the lower extremities and may be weeks or months old before they break free and embolize to the lungs.

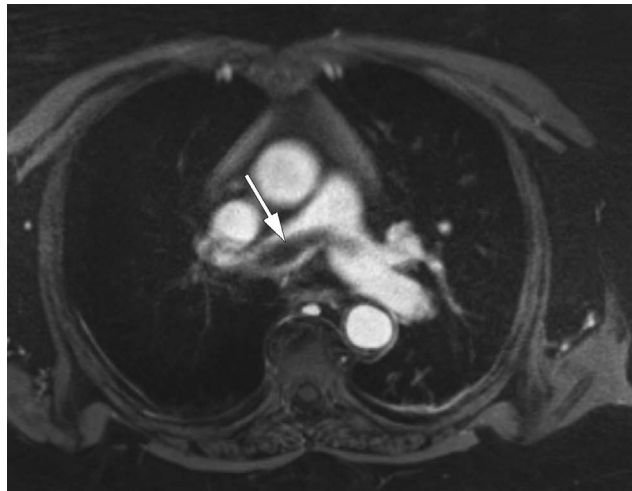


Fig 31-2. Acute pulmonary embolism (PE). Annotated. Chest. MRI. T1 weighted. Fat suppression. Contrast enhancement. Delayed phase. Axial plane. Motion-compensated sequence. There is a saddle PE (arrow). It is seen within the main pulmonary artery crossing over from its most prominent portion in the right pulmonary artery to the smaller portion seen in the left pulmonary artery.

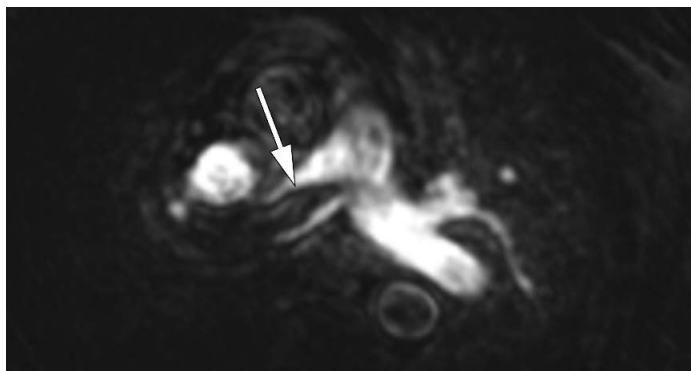


Fig 31-3. Acute PE. Annotated. Chest. MR angiography. Reformat. T1 weighted. Contrast enhancement. Axial plane. Arrow points to saddle PE predominantly in the right pulmonary artery.

Option B is not correct.

The filling defect is located centrally within the pulmonary artery. Chronic PE usually undergoes remodeling such that the clot is located eccentrically within the vessel, forming obtuse angles with the vessel wall.

Option C is not correct.

The filling defect does not enhance and is not expansile. Although acute PE can often be somewhat expansile, pulmonary artery sarcomas are usually quite expansile at presentation. They usually arise from the main pulmonary artery as well. Sarcomas would be expected to enhance; this lesion, a PE, does not.

Option D is not correct.

Tumor invading the pulmonary artery would be expected to enhance; this lesion does not. We would also expect to see an extravascular mass adjacent to the pulmonary artery, representing the invading tumor.

Reference(s):

Hochhegger B, Ley-Zaporozhan J, Marchiori E, et al. Magnetic resonance imaging findings in acute pulmonary embolism. *Br J Radiol.* 2011;84:282-287.

Kauczor HU, Schwickert HC, Mayer E, Kersjes W, Moll R, Schweden F. Pulmonary artery sarcoma mimicking chronic thromboembolic disease: computed tomography and magnetic resonance imaging findings. *Cardiovasc Intervent Radiol.* 1994;17:185-189.

Answer 32 is D.

Both focal nodular hyperplasia (FNH) and hepatocellular carcinoma (HCC) typically show robust enhancement on parenchymal arterial-phase sequences. FNH is similar to a hamartoma of the liver, composed of disorganized hepatocytes and bile ductules with intervening fibrous bands. Because of the similarity of FNH to background liver, it has been described as a “localized cirrhosis” on histopathology. FNH blends into the background hepatic parenchyma on precontrast T1-weighted sequences, and becomes isointense (or remains slightly hyperintense) to background liver on delayed postcontrast images. In contrast, HCC is supplied almost exclusively by the hepatic artery, typically without any portal vascular supply. On delayed-phase images, HCC “washes out” (ie, becomes hypointense to background liver parenchyma) because of this lack of portal supply, while the background liver becomes progressively brighter through a combination of the dominant portal blood flow and also from delayed enhancement of the fibrotic bands of the diseased liver.

Option A is not correct.

FNH is typically near isointense to background liver on precontrast T1-weighted images. HCC has a variable appearance on T1-weighted images and may present as hypointense, isointense, or slightly hyperintense to background hepatic parenchyma.

Option B is not correct.

Both FNH and HCC show arterial enhancement. FNH shows more consistent, avid enhancement in a properly timed arterial-phase sequence, with a characteristic internal architecture of small nodules. HCC typically displays more heterogeneous arterial enhancement and may show a “nodule-in-nodule” pattern, but this may not be distinctive from the internal architecture characteristic of an FNH.

Option C is not correct.

Though more typical of FNH, HCC may demonstrate a central scar. In addition, FNH does not always demonstrate a central scar.